

The gluon content of the η and η' mesons and the $\eta\gamma$, $\eta'\gamma$ electromagnetic transition form factors

S. S. Agaev*

*High Energy Physics Lab., Baku State University,
Z. Khalilov St. 23, 370148 Baku, Azerbaijan*

N. G. Stefanis†

*Institut für Theoretische Physik II,
Ruhr-Universität Bochum, D-44780 Bochum, Germany*
(Dated: February 8, 2020)

Abstract

We compute power-suppressed corrections $\sim 1/Q^{2n}$, $n = 1 \div 4$ to the $\eta\gamma$ and $\eta'\gamma$ transition form factors $Q^2 F_{\eta(\eta')\gamma}(Q^2)$ using the QCD running-coupling method combined with the infrared-renormalon calculus. The contribution to the form factors from the quark and gluon content of the η , η' mesons is taken into account, using for the $\eta - \eta'$ mixing the $SU_f(3)$ singlet η_1 and octet η_8 basis. The obtained theoretical predictions are compared with the corresponding CLEO data and restrictions on the input parameters (Gegenbauer coefficients) $B_2^q(\eta_1)$, $B_2^q(\eta_1)$, and $B_2^q(\eta_8)$ in the distribution amplitudes for the η_1 , η_8 states with one non-asymptotic term are deduced. Comparison is made with the results from QCD perturbation theory.

PACS numbers: 12.38.Bx, 11.10.Hi, 11.10.Jj, 14.40.Aq

*Electronic address: agaev.shahin@yahoo.com

†Electronic address: stefanis@tp2.ruhr-uni-bochum.de

I. INTRODUCTION

The electromagnetic transition form factors (FF's) $F_{M\gamma}(Q^2)$ of light pseudoscalar $M \equiv \pi^0, \eta, \eta'$ mesons were the subject of much theoretical [1, 2, 3, 4, 5, 6, 7, 8, 9, 10] and experimental [11] research in recent years. For instance, the CLEO collaboration reported about rather precise measurements of the $\pi^0\gamma$, $\eta\gamma$ and $\eta'\gamma$ transition FF's, stimulating interesting theoretical investigations aiming to account for the obtained experimental data within the framework of perturbative QCD (pQCD). The objective of such analyses is to model the π^0 , η and η' mesons distribution amplitudes (DA's) and, in the η , η' case, to extract some information on their gluon components.

Indeed, it is known that the physical η and η' mesons can be represented as superpositions of a flavor $SU_f(3)$ singlet η_1 and octet η_8 state

$$\begin{aligned} |\eta\rangle &= \cos\theta_p|\eta_8\rangle - \sin\theta_p|\eta_1\rangle, \\ |\eta'\rangle &= \sin\theta_p|\eta_8\rangle + \cos\theta_p|\eta_1\rangle. \end{aligned} \quad (1)$$

Unlike the octet η_8 state, the $SU_f(3)$ singlet η_1 contains a two-gluon component [12], which even absent at the normalization point μ_0^2 , appears in the region $Q^2 > \mu_0^2$ owing to quark-gluon mixing and renormalization-group evolution of the η_1 state DA. The η and η' mesons (cf. Eq. (1)) receive a gluon contribution due to the gluon content of the η_1 state. Because the meson-photon transition at leading order (LO) is a pure electromagnetic process, the gluon components of the η and η' mesons can directly contribute to the $\eta\gamma$ and $\eta'\gamma$ transitions only at next-to-leading order (NLO) due to quark box diagrams. They also affect the LO result through evolution of the quark component of the η , η' meson DA's. Contributions to the $\eta\gamma$ and $\eta'\gamma$ transition FF's, originating from the gluon content of the η and η' mesons, were recently computed [6] within the framework of the hard-scattering approach (HSA) of pQCD and estimates of the expansion parameters in the meson DA's were given.

The gluon contributions for the $\eta\gamma$ and $\eta'\gamma$ electromagnetic transition FF's are subdominant. But in some exclusive processes, like the B meson two-body non-leptonic exclusive and semi-inclusive decays, which involve the η and η' mesons, their gluon contribution can potentially play an essential role in explaining the experimental data (see Ref. [13] and references cited therein). The reason is that in these processes the gluon component of the η and η' mesons contributes to corresponding hard-scattering amplitudes already at LO of pQCD. Hence, the gluonic parts of the η , η' meson DA's, deduced from the $\eta\gamma$, $\eta'\gamma$ data, are important input ingredients in studying a wide range of exclusive processes, given that they are universal, i.e., process-independent quantities.

The HSA and the pQCD factorization theorems [14], at asymptotically large values of the momentum transfer Q^2 , lead to reliable predictions for exclusive processes. But in the momentum-transfer regime of a few GeV^2 , experimentally accessible at present for most exclusive processes, power-suppressed corrections $(1/Q^2)^p$, $p = 1, 2, 3 \dots$ may play an important role in explaining the experimental data. In order to evaluate such corrections, the QCD running-coupling (RC) method, combined with the infrared-renormalon (IR) calculus, was proposed [1, 2, 13, 15, 16]. This method allows one to evaluate power-behaved contributions in exclusive processes arising from the end-point regions $x \rightarrow 0, 1$. In this manner, power corrections to the electromagnetic FF's $F_M(Q^2)$ ($M \equiv \pi, K$) [15, 16], to the transition FF's $F_{M\gamma}(Q^2)$ ($M \equiv \pi^0, \eta, \eta'$) [1, 2], as well as to the gluon-gluon- η' vertex function [13] were computed. Power corrections can also be obtained by means of the Landau-pole free expression for the QCD coupling constant [17]. This analytic approach was used to

calculate in a unifying way power corrections to the electromagnetic pion FF and such to the inclusive cross section of the Drell-Yan process [18, 19].

Power corrections to the $\eta\gamma$ and $\eta'\gamma$ electromagnetic transition FF's within the RC method were computed in Ref. [1] and predictions for the structure of the DA's of the η and η' mesons were made. In the present work we extend this sort of investigation by also including into the calculation of the $\eta\gamma$, $\eta'\gamma$ transition FF's the leading power corrections originating from the gluonic content of the η , η' mesons that were not taken into account in Ref. [1]. This will enable us to extract their DA's from comparing our theoretical predictions with the CLEO data [11].

The paper is structured as follows: Sect. II contains all required information on the hard-scattering amplitudes for the $\eta_1\gamma$ and $\eta_8\gamma$ transitions, accounting also for the gluon content of the η_1 state. The DA's of the $SU_f(3)$ singlet η_1 and octet η_8 states are considered and their evolution is taken into account. In Sect. III we compute the $\eta\gamma$ and $\eta'\gamma$ transition FF's within the RC method and obtain the Borel resummed expressions for them. The asymptotic limit $Q^2 \rightarrow \infty$ of these FF's is explored and the standard HSA leading-twist predictions for the FF's are recovered. In Sect. IV we perform a numerical analysis and compare our results with the CLEO [11] data with the aim to extract constraints on the η and η' meson DA's. Finally, Sect. V contains our concluding remarks.

II. $SU_f(3)$ SINGLET AND OCTET COMPONENTS OF THE $\eta\gamma$, $\eta'\gamma$ TRANSITION FF'S

The meson-photon electromagnetic transition FF $F_{M\gamma}(Q^2)$ can be defined in terms of the invariant amplitude Γ^μ of the process¹

$$\gamma^*(q_1) + \gamma(q_2) \rightarrow M(p) \quad (2)$$

in the following way

$$\Gamma^\mu = ie^2 F_{M\gamma}(Q^2) \epsilon^{\mu\nu\alpha\beta} \epsilon_\nu(q_2) q_{1\alpha} q_{2\beta}, \quad (3)$$

where $\epsilon_\nu(q_2)$ is the polarization vector of the real photon and $Q^2 = -q_1^2$. The FF's of the $\eta\gamma$ and $\eta'\gamma$ transitions are sums of the corresponding singlet $F_{M\gamma}^1(Q^2)$ and octet $F_{M\gamma}^8(Q^2)$ contributions

$$F_{M\gamma}(Q^2) = F_{M\gamma}^1(Q^2) + F_{M\gamma}^8(Q^2). \quad (4)$$

The FF of the octet state $F_{M\gamma}^8(Q^2)$ and the quark-related component of the FF of the singlet state, $F_{M\gamma}^1(Q^2)$, can be computed by employing the results obtained for the pion-photon transition FF [6, 20]. The latter is known at $O(\alpha_s)$ of pQCD [20]. More recently, also a part of $O(\alpha_s^2)$ corrections were computed [21]. The gluonic component of the singlet contribution $F_{M\gamma}^1(Q^2)$ was just recently calculated within the framework of the HSA of pQCD in Ref. [6].

In accordance with the pQCD factorization theorems, at large momentum transfer, the FF's $F_{M\gamma}^1(Q^2)$ and $F_{M\gamma}^8(Q^2)$ can be represented in the form of a convolution of the corresponding hard-scattering amplitudes with the quark and gluon components of the DA's of the η_1 and η_8 states,

$$Q^2 F_{M\gamma}^1(Q^2) = f_M^1 N_1 \left\{ T_{H,0}^q(x) \otimes \phi_{\eta_1}^q(x, \mu_F^2) + \right.$$

¹ Hereafter M denotes the η or η' meson.

$$\frac{\alpha_s(\mu_R^2)}{4\pi} C_F \left[T_{H,1}^q(x, Q^2, \mu_F^2) \otimes \phi_{\eta_1}^q(x, \mu_F^2) + T_{H,1}^g(x, Q^2, \mu_F^2) \otimes \phi_{\eta_1}^g(x, \mu_F^2) \right] \} \quad (5)$$

and

$$Q^2 F_{M\gamma}^8(Q^2) = f_M^8 N_8 \left[T_{H,0}^q(x) \otimes \phi_{\eta_8}(x, \mu_F^2) + \frac{\alpha_s(\mu_R^2)}{4\pi} C_F T_{H,1}^q(x, Q^2, \mu_F^2) \otimes \phi_{\eta_8}(x, \mu_F^2) \right], \quad (6)$$

where all quantities above are renormalized, i.e., singularity-free, and the symbol \otimes denotes the convolution

$$T_H(x) \otimes \phi(x) = \int_0^1 dx T_H(x) \phi(x).$$

Here the functions $T_{H,0}^q(x)$ and $T_{H,1}^q(x, Q^2, \mu_F^2)$ are hard-scattering amplitudes for the partonic subprocess $\gamma + \gamma^* \rightarrow q + \bar{q}$ at LO and NLO, respectively, and $T_{H,1}^g(x, Q^2, \mu_F^2)$ is the NLO hard-scattering amplitude for $\gamma + \gamma^* \rightarrow g + g$. In Eqs. (5) and (6), f_M^i are the M -meson decay constants, $C_F = 4/3$ is the color factor, and N_1 and N_8 are numerical constants each depending on the quark structure of the associated η_1 , η_8 state. Because the $SU_f(3)$ singlet η_1 and octet η_8 states have the quark-antiquark decompositions

$$|\eta_1\rangle = \frac{1}{\sqrt{3}}|u\bar{u} + d\bar{d} + s\bar{s}\rangle, \quad |\eta_8\rangle = \frac{1}{\sqrt{6}}|u\bar{u} + d\bar{d} - 2s\bar{s}\rangle, \quad (7)$$

the constants N_1 and N_8 are given by the expressions

$$N_1 = \frac{1}{\sqrt{3}}(e_u^2 + e_d^2 + e_s^2), \quad N_8 = \frac{1}{\sqrt{6}}(e_u^2 + e_d^2 - 2e_s^2). \quad (8)$$

The hard-scattering amplitudes $T_{H,0}^q(x)$, $T_{H,1}^q(x, Q^2, \mu_F^2)$, and $T_{H,1}^g(x, Q^2, \mu_F^2)$ are well known [6, 20, 21] and are given by the following expressions

$$\begin{aligned} T_{H,0}^q(x) &= \frac{1}{x} + \frac{1}{\bar{x}}, \\ T_{H,1}^q(x, Q^2, \mu_F^2) &= \frac{1}{x} \left[\ln^2 x - \frac{x \ln x}{\bar{x}} - 9 \right] + \frac{1}{x} (3 + 2 \ln x) \ln \frac{Q^2}{\mu_F^2} + (x \leftrightarrow \bar{x}), \\ T_{H,1}^g(x, Q^2, \mu_F^2) &= \frac{x \ln^2 x}{\bar{x}} + \left(6 - \frac{4}{\bar{x}} \right) \ln x + 2 \frac{x \ln x}{\bar{x}} \ln \frac{Q^2}{\mu_F^2} - (x \leftrightarrow \bar{x}), \end{aligned} \quad (9)$$

where $\bar{x} \equiv 1 - x$. For our purposes below it is convenient to adopt the so-called default choice and set the factorization scale μ_F^2 in Eqs. (5), (6) and (9) equal to the external large momentum scale Q^2 , a choice that eliminates terms $\sim \ln(Q^2/\mu_F^2)$ in the hard-scattering amplitudes, simplifying them considerably.

The next ingredients needed for computing the FF's $F_{M\gamma}^1(Q^2)$ and $F_{M\gamma}^8(Q^2)$ are the meson-decay constants f_M^i and the distribution amplitudes $\phi_{\eta_1}^q(x, Q^2)$, $\phi_{\eta_1}^g(x, Q^2)$, and $\phi_{\eta_8}(x, Q^2)$ for the η_1 , η_8 states. The decay constants f_M^i are defined as the matrix elements of the axial-vector currents $J_{\mu 5}^i$ with $i = 1, 8$

$$\langle 0 | J_{\mu 5}^i | M(p) \rangle = i f_M^i p_\mu. \quad (10)$$

In the octet-singlet basis the constants f_M^i can be parameterized by two methods. One is to follow the pattern of state mixing (cf. Eq. 1))

$$f_\eta^8 = f_8 \cos \theta_p, \quad f_\eta^1 = -f_1 \sin \theta_p,$$

$$f_{\eta'}^8 = f_8 \sin \theta_p, \quad f_{\eta'}^1 = f_1 \cos \theta_p, \quad (11)$$

where the decay constants f_1 , f_8 and θ_p are given by [22]

$$f_1 = 1.17 f_\pi, \quad f_8 = 1.26 f_\pi, \quad \theta_p = -15.4^\circ \quad (12)$$

with $f_\pi = 0.131$ GeV being the pion decay constant.

The second method employs a two-mixing angles parameterization:

$$\begin{aligned} f_\eta^8 &= f_8 \cos \theta_8, \quad f_\eta^1 = -f_1 \sin \theta_1, \\ f_{\eta'}^8 &= f_8 \sin \theta_8, \quad f_{\eta'}^1 = f_1 \cos \theta_1 \end{aligned} \quad (13)$$

with the mixing angles θ_1 and θ_8 given by [22]

$$\theta_1 = -9.2^\circ, \quad \theta_8 = -21.2^\circ. \quad (14)$$

It is worth noting that parameterization (11) leads to simple expressions for the physical FF's in terms of the $F_{\eta_1\gamma}(Q^2)$ and $F_{\eta_8\gamma}(Q^2)$ ones; viz.,

$$\begin{aligned} F_{\eta\gamma}(Q^2) &= \cos \theta_p F_{\eta_8\gamma}(Q^2) - \sin \theta_p F_{\eta_1\gamma}(Q^2), \\ F_{\eta'\gamma}(Q^2) &= \sin \theta_p F_{\eta_8\gamma}(Q^2) + \cos \theta_p F_{\eta_1\gamma}(Q^2), \end{aligned} \quad (15)$$

where the form factors $F_{\eta_1\gamma}(Q^2)$ and $F_{\eta_8\gamma}(Q^2)$ are determined by expressions (5) and (6), but with f_M^i replaced by f_i . Note that in our numerical computations we shall use both the conventional one-angle mixing scheme and the two mixing-angles parameterization.

The main question still to be answered concerns the shape of the DA's of the η_1 and η_8 states. In general, a meson DA is a function containing all non-perturbative, long-distance effects, which cannot be calculated by employing perturbative QCD methods. Nonetheless, as a direct consequence of factorization, the evolution of the DA with the factorization scale μ_F^2 is governed by pQCD. Input information at the starting point of evolution, i.e., the dependence of the DA on the variable x , has to be extracted from experimental data or found by using non-perturbative methods, for example, QCD sum rules with nonlocal condensates [23] (see also [24]) or instanton-based models [25] at some (low) momentum scale characteristic for the particular nonperturbative model.

Due to mixing of the quark-antiquark component with the two-gluon part of the DA, the evolution equation for the DA of the flavor singlet pseudoscalar η_1 state has a 2×2 matrix form [12]. The solution of this equation is given by the expressions

$$\phi^q(x, Q^2) = 6x\bar{x} \left\{ 1 + \sum_{n=2,4..}^{\infty} \left[B_n^q \left(\frac{\alpha_s(\mu_0^2)}{\alpha_s(Q^2)} \right)^{\frac{\gamma_+^n}{\beta_0}} + \rho_n^q B_n^g \left(\frac{\alpha_s(\mu_0^2)}{\alpha_s(Q^2)} \right)^{\frac{\gamma_-^n}{\beta_0}} \right] C_n^{3/2}(x - \bar{x}) \right\} \quad (16)$$

and

$$\phi^g(x, Q^2) = x\bar{x} \sum_{n=2,4..}^{\infty} \left[\rho_n^q B_n^q \left(\frac{\alpha_s(\mu_0^2)}{\alpha_s(Q^2)} \right)^{\frac{\gamma_+^n}{\beta_0}} + B_n^g \left(\frac{\alpha_s(\mu_0^2)}{\alpha_s(Q^2)} \right)^{\frac{\gamma_-^n}{\beta_0}} \right] C_{n-1}^{5/2}(x - \bar{x}). \quad (17)$$

Here $C_n^{3/2}(z)$ and $C_n^{5/2}(z)$ are Gegenbauer polynomials. Detailed information concerning the parameters ρ_n^q , ρ_n^g and the anomalous dimensions γ_+^n , γ_-^n can be found in Ref. [13]. In Eqs.

(16) and (17) the coefficients B_n^q and B_n^g will be considered as free input parameters, the values of which at the normalization point μ_0^2 determine the shapes of the DA's $\phi^q(x, Q^2)$ and $\phi^g(x, Q^2)$.

In our calculations we shall use the DA for the η_1 state containing only the first Gegenbauer polynomials $C_2^{3/2}(x - \bar{x})$ and $C_1^{5/2}(x - \bar{x})$ (i.e., $B_2^q \neq 0$, $B_2^g \neq 0$ and $B_n^q = B_n^g = 0$ for all $n > 2$)

$$C_2^{3/2}(x - \bar{x}) = 6(1 - 5x\bar{x}), \quad C_1^{5/2}(x - \bar{x}) = 5(x - \bar{x}). \quad (18)$$

Under this assumption the DA's assume the following forms [13]

$$\begin{aligned} \phi_{\eta_1}^q(x, Q^2) &= 6x\bar{x} \left[1 + A(Q^2) - 5A(Q^2)x\bar{x} \right], \\ \phi_{\eta_1}^g(x, Q^2) &= x\bar{x}(x - \bar{x})B(Q^2). \end{aligned} \quad (19)$$

The functions $A(Q^2)$ and $B(Q^2)$ are defined by

$$\begin{aligned} A(Q^2) &= 6B_2^q \left(\frac{\alpha_s(Q^2)}{\alpha_s(\mu_0^2)} \right)^{\frac{48}{81}} - \frac{B_2^g}{15} \left(\frac{\alpha_s(Q^2)}{\alpha_s(\mu_0^2)} \right)^{\frac{101}{81}}, \\ B(Q^2) &= 16B_2^q \left(\frac{\alpha_s(Q^2)}{\alpha_s(\mu_0^2)} \right)^{\frac{48}{81}} + 5B_2^g \left(\frac{\alpha_s(Q^2)}{\alpha_s(\mu_0^2)} \right)^{\frac{101}{81}}. \end{aligned} \quad (20)$$

The DA of the octet η_8 state contains only the quark component $\phi_{\eta_8}(x, Q^2)$. This DA is identical to the $\phi_{\eta_1}^q(x, Q^2)$, but with $A(Q^2)$ replaced by $C(Q^2)$, i.e.,

$$C(Q^2) = 6B_2^q \left(\frac{\alpha_s(Q^2)}{\alpha_s(\mu_0^2)} \right)^{\frac{50}{81}}. \quad (21)$$

The numerical values of the anomalous dimensions γ_+^2 , γ_-^2 in Eq. (20) and γ_2 in Eq. (21) are presented for $n_f = 3$. If necessary, we shall distinguish between input parameters in Eqs. (20) and (21) using the notation $B_2^q(\eta_1)$ and $B_2^q(\eta_8)$.

III. BOREL RESUMMED $\eta\gamma$ AND $\eta'\gamma$ TRANSITION FF'S

In Sect. II we have outlined the key ingredients pertaining to both the standard HSA as well as the RC treatment of the transition FF's $F_{M\gamma}^1(Q^2)$ and $F_{M\gamma}^8(Q^2)$. Let us now turn to a discussion of the main differences between these two approaches, starting with the choice of the scales μ_R^2 and μ_F^2 . It is evident that if a physical quantity can be factorized, like Eqs. (5) and (6), then the LHS cannot depend on artificial intrinsic scales or on the particular renormalization and factorization schemes adopted. But at any finite order of QCD perturbation theory, truncation of the corresponding perturbative series will give rise to a dependence on the scales μ_F^2 and μ_R^2 , as well as on the factorization and renormalization scheme (for an in-depth discussion of these issues, we refer the reader to the second paper of Ref. [5]). Because higher-order corrections in pQCD computations are, as a rule, large for both inclusive and exclusive processes, reliable theoretical predictions require an optimal scale setting that minimizes higher-order corrections. Typically, the factorization scale enters the NLO contribution to the hard-scattering amplitude of meson transition or electromagnetic form

factors in the form $\sim \ln(Q^2/\mu_F^2)$, so that taking μ_F^2 equal to Q^2 eliminates this term. This scale setting has been used in Sect. II.

The choice of the renormalization scale is somewhat subtler because this scale enters not only the NLO contribution, but also as the argument of the running strong coupling $\alpha_s(\mu_R^2)$. To discuss this question, consider first the scale of the strong coupling. One effective method to solve this problem is the Brodsky-Lepage-Mackenzie (BLM) scale-setting procedure [26]. In the framework of this method a large part of the higher-order corrections—namely, those originating from the quark vacuum diagrams (quark “bubbles”)—can be absorbed into the scale of the QCD coupling constant. When utilizing this new scale one finds the NLO correction significantly reduced relative to its initial value. The generalization of the BLM procedure to all orders of pQCD led to the invention of the RC method and the IR renormalon calculus (for a review, see Ref. [27]). In the case of inclusive processes, it was proven by explicit calculation that all-order resummation of diagrams with a chain of (quark) bubble insertions into the gluon line gives the same results as the calculation of one-loop Feynman diagrams for the quantity under consideration using the QCD running coupling at the vertices. Moreover, the IR renormalon calculus in conjunction with the “ultraviolet dominance hypothesis” enables one to estimate power-suppressed (e.g., higher-twist) corrections to a wide range of inclusive processes.²

This approach was used for studying IR renormalon effects in exclusive processes as well. For instance, $(-\beta_0 \alpha_s/4\pi)^n$ corrections to the Brodsky-Lepage evolution kernel $V[x, y; \alpha_s(Q^2)]$ were computed in Ref. [28, 29] and renormalon chain contributions to the pseudoscalar meson DA and the $\pi^0\gamma$ transition FF were taken into account in [28]. Similar investigations along this line of thought were performed in Refs. [30, 31].

In addition to loop-integration ambiguities, exclusive processes may receive power-behaved contributions due to the choice of the renormalization scale. In fact, in order to reduce the NLO correction, for example, to the pion electromagnetic FF $F_\pi(Q^2)$, the renormalization scale μ_R^2 should be set equal to the typical four-momentum, flowing through hard gluon lines in the partonic subprocess $q\bar{q}' + \gamma^* \rightarrow q\bar{q}'$ [26]. Choosing the scale μ_R^2 this way inevitably leads to a dependence on the longitudinal momentum fractions carried by the hadron’s constituents. In the case of $F_\pi(Q^2)$, the NLO contribution to the hard-scattering amplitude $T_H^1(x, y, Q^2)$ contains a logarithm of the form $\ln(\mu_R^2/\bar{x}\bar{y}Q^2)$, with x and y being, respectively, the longitudinal momentum fractions of the quarks in the initial and the final pion. Hence, the natural choice to eliminate this term would be to set $\mu_R^2 = \bar{x}\bar{y}Q^2$. But due to the convolution of the hard and soft contribution (cf. e.g., Eq. (5)), integrations over x and y appear that give rise to power corrections when approaching the end-point $x \rightarrow 0, 1$; $y \rightarrow 0, 1$ regions. Renormalizing the process amplitude at a scale close to the large external momentum Q^2 makes such contributions less pronounced but at the expense of large NLO logarithms. Therefore, if we are to optimize our theoretical calculation, we have to minimize NLO contributions while keeping under control power corrections in the end-point regions.

Specifically, for the meson-photon transition we have $\mu_R^2 = Q^2x$ and $\bar{\mu}_R^2 = Q^2\bar{x}$ because in the corresponding two, leading-order, Feynman diagrams the absolute values of the square of the momenta flowing through virtual quark lines are determined exactly by these expressions. In the standard HSA one “freezes” the scale of the QCD coupling constant μ_R^2 ($\bar{\mu}_R^2$), by

² We consider the one-loop integration with the QCD running coupling as one possible “source” of power corrections.

replacing x by its mean value $\langle x \rangle = 1/2$ and performs then the integrations in Eqs. (5) and (6) with $\alpha_s(Q^2/2)$. Within the context of the RC method we express the running coupling $\alpha_s(\lambda Q^2)$ in terms of $\alpha_s(Q^2)$ by means of the renormalization-group equation and perform the integration over x using the principal value prescription. The final result of this procedure is the Borel resummed FF $[Q^2 F_{M\gamma}(Q^2)]^{res}$ that contains power corrections from the end-point regions. These corrections are implicitly contained in the pQCD factorization formulas (5) and (6) but cannot be accounted for in the standard HSA when freezing the renormalization scale μ_R^2 and ignoring its dependence on the longitudinal momentum fractions (though this scale choice is perfectly legitimate).

After this general discussion, let us turn to Eqs. (5) and (6). First, consider the standard treatment of these expressions. We concentrate on the NLO corrections $\sim \alpha_s(\mu_R^2)$ and, for simplicity, restrict our consideration only to the quark component of Eq. (5). The generalization of our analysis to encompass the gluon component of the FF is straightforward.

Omitting an unimportant, in the present context, constant factor, we get

$$\begin{aligned} Q^2 F_{M\gamma}^1(Q^2)_1^{quark} \sim \alpha_s(\mu_R^2) t(x) \otimes \phi_{\eta_1}^q(x, Q^2) + \alpha_s(\mu_R^2) t(\bar{x}) \otimes \phi_{\eta_1}^q(x, Q^2) = \\ 2\alpha_s(\mu_R^2) t(x) \otimes \phi_{\eta_1}^q(x, Q^2), \end{aligned} \quad (22)$$

where the function $t(x)$ is

$$t(x) = \frac{1}{x} \left[\ln^2 x - \frac{x \ln x}{\bar{x}} - 9 \right]. \quad (23)$$

In deriving Eq. (22) we used the symmetry property of the quark component of the η_1 state DA, valid also for the function $\phi_{\eta_8}(x, Q^2)$,

$$\phi_{\eta_1}^q(x, Q^2) = \phi_{\eta_1}^q(\bar{x}, Q^2), \quad \phi_{\eta_8}(x, Q^2) = \phi_{\eta_8}(\bar{x}, Q^2). \quad (24)$$

The generalization of Eq. (22) within the RC method can be achieved by setting $\mu_R^2 = Q^2 x$ in the term $\sim t(x)$ and equating it to $Q^2 \bar{x}$ in the second term $\sim t(\bar{x})$ [1, 2]. Hence, we obtain

$$\begin{aligned} Q^2 F_{M\gamma}^1(Q^2)_1^{quark} \sim \alpha_s(Q^2 x) t(x) \otimes \phi_{\eta_1}^q(x, Q^2) + \alpha_s(Q^2 \bar{x}) t(\bar{x}) \otimes \phi_{\eta_1}^q(x, Q^2) = \\ 2\alpha_s(Q^2 x) t(x) \otimes \phi_{\eta_1}^q(x, Q^2). \end{aligned} \quad (25)$$

After a similar analysis for the gluon component of the form factor $Q^2 F_{M\gamma}^1(Q^2)$ within the RC method, we find

$$Q^2 F_{M\gamma}^1(Q^2)_1^{gluon} \sim 2\alpha_s(Q^2 x) g(x) \otimes \phi_{\eta_1}^g(x, Q^2), \quad (26)$$

whereas the result in the HSA framework is the same with the argument of α_s replaced by μ_R^2 and the function $g(x)$ is given by the expression

$$g(x) = \frac{x \ln^2 x}{\bar{x}} + \left(6 - \frac{4}{\bar{x}} \right) \ln x \quad (27)$$

making use of the antisymmetry of the gluon DA $\phi_{\eta_1}^g(x, Q^2)$ under the exchange $x \leftrightarrow \bar{x}$

$$\phi_{\eta_1}^g(x, Q^2) = -\phi_{\eta_1}^g(\bar{x}, Q^2). \quad (28)$$

Summing up, we can write the transition FF's $Q^2 F_{M\gamma}^1(Q^2)$ and $Q^2 F_{M\gamma}^8(Q^2)$ in the context of the RC method as follows

$$Q^2 F_{M\gamma}^1(Q^2) = f_M^1 N_1 \left\{ T_{H,0}^q(x) \otimes \phi_{\eta_1}^q(x, Q^2) + \frac{C_F}{2\pi} \left[\alpha_s(Q^2 x) t(x) \otimes \phi_{\eta_1}^q(x, Q^2) + \alpha_s(Q^2 x) g(x) \otimes \phi_{\eta_1}^g(x, \mu_F^2) \right] \right\} \quad (29)$$

and

$$Q^2 F_{M\gamma}^8(Q^2) = f_M^8 N_8 \left[T_{H,0}^q(x) \otimes \phi_{\eta_8}(x, Q^2) + \frac{C_F}{2\pi} \alpha_s(Q^2 x) t(x) \otimes \phi_{\eta_8}(x, Q^2) \right]. \quad (30)$$

In order to perform the integrations with the running coupling $\alpha_s(Q^2 x)$, we need its expression in terms of $\alpha_s(Q^2)$. Because in Eqs. (16) and (17) we shall use the two-loop approximation for the running coupling $\alpha_s(Q^2)$

$$\alpha_s(Q^2) = \frac{4\pi}{\beta_0 \ln(Q^2/\Lambda^2)} \left[1 - \frac{2\beta_1}{\beta_0^2} \frac{\ln \ln(Q^2/\Lambda^2)}{\ln(Q^2/\Lambda^2)} \right], \quad (31)$$

with β_0 and β_1 being the one- and two-loop coefficients, respectively, of the QCD beta function

$$\beta_0 = 11 - \frac{2}{3} n_f, \quad \beta_1 = 51 - \frac{19}{3} n_f,$$

the expression for $\alpha_s(Q^2 x)$ should be taken with the same accuracy [1, 13], i.e.,

$$\alpha_s(Q^2 x) = \frac{4\pi}{\beta_0} \int_0^\infty du e^{-ut} R(u, t) x^{-u}. \quad (32)$$

Here $t = 4\pi/\beta_0 \alpha_s(Q^2)$ and the function $R(u, t)$ is defined as

$$R(u, t) = 1 - \frac{2\beta_1}{\beta_0^2} u (1 - \gamma_E - \ln t - \ln u), \quad (33)$$

where $\gamma_E \simeq 0.577216$ is the Euler constant.

Having used Eqs. (19), (23), (27) and (32) in Eqs. (29) and (30) and performing the integrations over x , we then find the FF's $Q^2 F_{M\gamma}^1(Q^2)$ and $Q^2 F_{M\gamma}^8(Q^2)$ within the RC method; viz.,

$$Q^2 F_{M\gamma}^1(Q^2) = f_M^1 N_1 \left\{ 6 + A(Q^2) + \frac{12C_F}{\beta_0} \left[(1 + A(Q^2)) \int_0^\infty du e^{-ut} R(u, t) Q_1(u) - 5A(Q^2) \int_0^\infty du e^{-ut} R(u, t) Q_2(u) \right] + \frac{2C_F}{\beta_0} B(Q^2) \int_0^\infty du e^{-ut} R(u, t) G(u) \right\} \quad (34)$$

and

$$Q^2 F_{M\gamma}^8(Q^2) = f_M^8 N_8 \left\{ 6 + C(Q^2) + \frac{12C_F}{\beta_0} \left[(1 + C(Q^2)) \int_0^\infty du e^{-ut} R(u, t) Q_1(u) - 5C(Q^2) \int_0^\infty du e^{-ut} R(u, t) Q_2(u) \right] \right\}. \quad (35)$$

The functions $Q_1(u)$, $Q_2(u)$ and $G(u)$ have the expressions

$$Q_1(u) = B(2, 1-u) \left[(\psi(1-u) - \psi(3-u))^2 + \psi'(1-u) - \psi'(3-u) \right] - \\ B(1, 2-u) [\psi(2-u) - \psi(3-u)] - 9B(1-u, 2), \quad (36)$$

$$Q_2(u) = B(3, 2-u) \left[(\psi(2-u) - \psi(5-u))^2 + \psi'(2-u) - \psi'(5-u) \right] - \\ B(2, 3-u) [\psi(3-u) - \psi(5-u)] - 9B(3, 2-u) \quad (37)$$

and

$$G(u) = B(1, 4-u) \left[(\psi(4-u) - \psi(5-u))^2 + \psi'(4-u) - \psi'(5-u) \right] + \\ 6B(2, 3-u) [\psi(3-u) - \psi(5-u)] - 4B(1, 3-u) [\psi(3-u) - \psi(4-u)] - \\ B(2, 3-u) \left[(\psi(3-u) - \psi(5-u))^2 + \psi'(3-u) - \psi'(5-u) \right] - \\ 6B(3, 2-u) [\psi(2-u) - \psi(5-u)] + 4B(2, 2-u) [\psi(2-u) - \psi(4-u)], \quad (38)$$

where the standard notations for the special functions $B(x, y)$, $\psi(z)$ and $\psi'(z)$

$$B(x, y) = \frac{\Gamma(x)\Gamma(y)}{\Gamma(x+y)}, \quad \psi(z) = \frac{d \ln \Gamma(z)}{dz}, \quad \psi'(z) = \frac{d\psi(z)}{dz} \quad (39)$$

are employed.

These somewhat cumbersome and for the further analysis unsuitable expressions can be considerably simplified by making use of [32]

$$\psi(z+n) = \psi(z) + \sum_{k=0}^{n-1} \frac{1}{k+z}, \quad \psi'(z+n) = \psi'(z) - \sum_{k=0}^{n-1} \frac{1}{(k+z)^2}. \quad (40)$$

Furthermore, the functions $Q_1(u)$, $Q_2(u)$ and $G(u)$ can be recast into the forms

$$Q_1(u) = \frac{2}{(1-u)^3} - \frac{2}{(2-u)^3} + \frac{1}{(2-u)^2} - \frac{9}{(1-u)(2-u)}, \\ Q_2(u) = \frac{2}{(2-u)^3} - \frac{4}{(3-u)^3} + \frac{2}{(4-u)^3} + \frac{1}{(3-u)^2} - \\ \frac{1}{(4-u)^2} - \frac{18}{(2-u)(3-u)(4-u)}, \\ G(u) = \frac{4}{(4-u)^3} - \frac{2}{(3-u)^3} + \frac{2}{(2-u)^2} - \frac{10}{(3-u)^2} + \frac{12}{(4-u)^2}. \quad (41)$$

One observes that the FF's given by (34) and (35) contain a finite number of triple and single poles located at the points $u_0 = 1, 2, 3, 4$, as well as double poles sitting at $u_0 = 2, 3, 4$. In other words, employing expression (32), we have transformed the end-point $x \rightarrow 0$ singularities in Eqs. (29) and (30) into (multiple) poles in the Borel plane u . These poles are the footprints of the IR renormalons and consequently the integrals in Eqs. (34) and (35) are just the inverse Borel transformations, in which the quark and gluon components of the Borel transforms $B[Q^2 F_{M\gamma}^{1(8)}](u)$ are proportional (up to constant factors) to the functions

$$R(u, t)Q_1(u), \quad R(u, t)Q_2(u), \quad R(u, t)G(u).$$

The IR renormalon divergences can be cured by employing the principal value prescription, which we adopt in this work to regularize divergent integrals. Therefore, the integrals over u in Eqs. (34) and (35) are to be understood in the sense of the Cauchy principal value. Removing these divergences, Eqs. (34) and (35) become the Borel resummed expressions $[Q^2 F_{M\gamma}^1(Q^2)]^{res}$ and $[Q^2 F_{M\gamma}^8(Q^2)]^{res}$ for these scaled FF's. It is known [1, 13] that the IR renormalon pole located at $u_0 = n$ corresponds to the power-suppressed correction $\sim (1/Q^2)^n$, contained in the scaled FF's. As a result, the scaled and resummed FF's contain power corrections $\sim (1/Q^2)^p$, $p = 1, 2, 3, 4$, which in the region of low Q^2 change their behavior as functions of Q^2 significantly, both qualitatively and quantitatively.

The principal value prescription, adopted here to regularize divergent integrals over u , generates higher-twist (HT) uncertainties

$$\sim N_q \frac{\Phi_q(Q^2)}{Q^{2q}},$$

where $\{\Phi_q(Q^2)\}$ are calculable functions entirely determined by the residues of the Borel transforms $B[Q^2 F_{M\gamma}^{1(8)}](u)$ at the pole $q = u_0$ and $\{N_q\}$ are arbitrary constants. Taking into account in Eqs. (34) and (35) these uncertainties modify the Borel resummed FF's, yielding

$$[Q^2 F_{M\gamma}^{1(8)}(Q^2)]^{res} \rightarrow [Q^2 F_{M\gamma}^{1(8)}(Q^2)]^{res} + [Q^2 F_{M\gamma}^{1(8)}(Q^2)]^{HT}. \quad (42)$$

In accordance with the “ultraviolet dominance hypothesis”, the HT uncertainty in Eq. (42) will allow us to estimate higher-twist corrections to the scaled FF's stemming from sources other than the end-point integrations. [For example, such originating from the η and η' mesons two-particle higher-twist DA's]. Indeed, by fitting the constants $\{N_q\}$ to the experimental data, one can deduce some information concerning the magnitude of such corrections.

It should be clear that regardless of the methods employed for the computation of the form factors, in the limit $Q^2 \rightarrow \infty$ these must reach their asymptotic values. The important problem to be clarified is then whether our resummed expressions $[Q^2 F_{\eta\gamma}(Q^2)]^{res}$, $[Q^2 F_{\eta'\gamma}(Q^2)]^{res}$ lead in the limit $Q^2 \rightarrow \infty$ to their corresponding well-known asymptotic forms. To answer this question, we first explore the $Q^2 \rightarrow \infty$ limits of the DA's $\phi_{\eta_1}^q(x, Q^2)$, $\phi_{\eta_1}^g(x, Q^2)$, and $\phi_{\eta_8}(x, Q^2)$. Since in Eqs. (16) and (17) the eigenvalues $\gamma_{\pm}^n < 0$ and their absolute values increase with n for all $n \geq 2$, in the asymptotic limit only the quark component of the η_1 state DA survives, evolving to its asymptotic form, whereas the DA of the gluon component $\phi_{\eta_1}^g(x, Q^2)$ in this limit vanishes, i.e.,

$$\phi_{\eta_1}^q(x, Q^2) \xrightarrow{Q^2 \rightarrow \infty} 6x\bar{x}, \quad \phi_{\eta_1}^g(x, Q^2) \xrightarrow{Q^2 \rightarrow \infty} 0.$$

The same arguments are valid also for the DA of the η_8 state, consisting only of the quark component

$$\phi_{\eta_8}(x, Q^2) \xrightarrow{Q^2 \rightarrow \infty} 6x\bar{x}.$$

In our case this means that the following limits are fulfilled

$$A(Q^2), \quad B(Q^2), \quad C(Q^2) \xrightarrow{Q^2 \rightarrow \infty} 0. \quad (43)$$

Moreover, we have to take into account that in this limit the term $\sim \alpha_s^2(Q^2)$ in the expansion of $\alpha_s(Q^2 x)$ in terms of $\alpha_s(Q^2)$ has to be neglected [1, 13]. The latter requirement is equivalent to the replacement

$$\int_0^{\infty} e^{-ut} R(u, t) du \rightarrow \int_0^{\infty} e^{-ut} du. \quad (44)$$

Then we obtain

$$[Q^2 F_{M\gamma}(Q^2)]^{res} \xrightarrow{Q^2 \rightarrow \infty} 6 \left(f_M^1 N_1 + f_M^8 N_8 \right) \left[1 + \frac{2C_F}{\beta_0} \int_0^\infty du e^{-ut} Q_1(u) \right]. \quad (45)$$

But this is not the final result because in the integral above $t = \ln(Q^2/\Lambda^2)$ and its $Q^2 \rightarrow \infty$ limit still has to be computed. The integral

$$\int_0^\infty du e^{-ut} \left[\frac{2}{(1-u)^3} - \frac{2}{(2-u)^3} + \frac{1}{(2-u)^2} - \frac{9}{1-u} + \frac{9}{2-u} \right] \quad (46)$$

can be expressed in terms of the logarithmic integral

$$li(x) = P.V. \int_0^x \frac{dt}{\ln t} \quad (47)$$

after performing an integration of the first three terms by parts to obtain

$$\int_0^\infty \frac{e^{-ut} du}{(n-u)^3} = -\frac{1}{2n^2} - \frac{\ln \lambda}{2n} + \frac{\ln^2 \lambda}{2} \frac{li(\lambda^n)}{\lambda^n}, \quad \int_0^\infty \frac{e^{-ut} du}{(n-u)^2} = -\frac{1}{n} + \ln \lambda \frac{li(\lambda^n)}{\lambda^n}, \quad (48)$$

where $\lambda = Q^2/\Lambda^2$. Now employing the formula [13]

$$\frac{li(x^n)}{x^n} \simeq \frac{1}{n \ln x} \sum_{m=0}^M \frac{m!}{(n \ln x)^m}, \quad M \gg 1,$$

and retaining in the expressions

$$\ln^2 \lambda \frac{li(\lambda^n)}{\lambda^n}, \quad \ln \lambda \frac{li(\lambda^n)}{\lambda^n}$$

terms up to $O(1/\ln \lambda)$ order, we finally find

$$\begin{aligned} [Q^2 F_{M\gamma}(Q^2)]^{res} &\xrightarrow{Q^2 \rightarrow \infty} 6 \left(f_M^1 N_1 + f_M^8 N_8 \right) \left[1 - \frac{5}{3\pi} \alpha_s(Q^2) \right] = \\ &\frac{1}{\sqrt{3}} \left(4f_M^1 + \sqrt{2}f_M^8 \right) \left[1 - \frac{5}{3\pi} \alpha_s(Q^2) \right]. \end{aligned} \quad (49)$$

It is worth noting that numerical constants and terms $\sim \ln \lambda$ in Eq. (46), appearing due to Eq. (48), cancel out in the final result.

Equation (49) for $M = \eta$ and η' supplies the asymptotic limit of the corresponding transition FF's. These limits can be readily obtained within the standard HSA by means of the asymptotic DA's of the η_1 and η_8 states. Stated differently, by explicit computation we have proved that in the $Q^2 \rightarrow \infty$ limit the Borel resummed expressions (34) and (35) lead to the well-known asymptotic forms of the $F_{\eta\gamma}(Q^2)$ and $F_{\eta'\gamma}(Q^2)$ form factors.

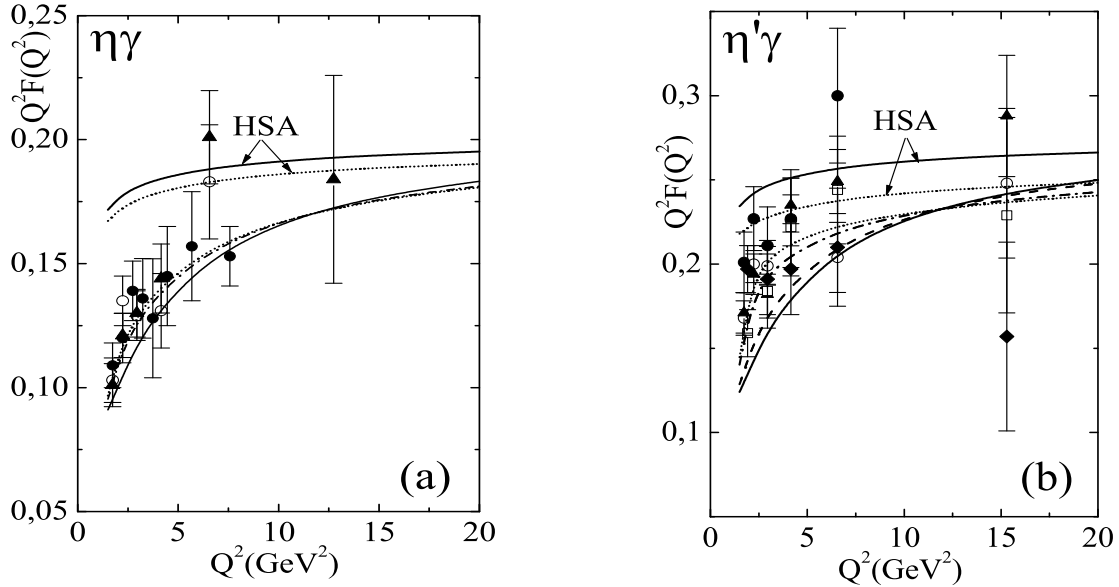


FIG. 1: Predictions for the scaled form factors as functions of Q^2 of the $\eta\gamma$ (left) and $\eta'\gamma$ (right) electromagnetic transition. The curves labelled HSA are computed within NLO perturbative QCD. All curves are obtained using for the η_1 and η_8 meson DA's the input parameters $B_2^g(\eta_1) = B_2^g(\eta_8) = 0$. For the solid curves the designation is $B_2^g(\eta_1) = 0$. The dashed curve on the RHS corresponds to $B_2^g(\eta_1) = 4$; for the dash-dotted curves we use $B_2^g(\eta_1) = 14$ and for the dotted ones $B_2^g(\eta_1) = 18$. The data are taken from Ref. [11].

IV. EXTRACTING THE η AND η' MESON DA'S

In this section we perform numerical computations of the Borel resummed $\eta\gamma$ and $\eta'\gamma$ transition FF's³ in order to extract the η and η' meson DA's from the CLEO data. Calculation of the same FF's within the standard HSA is also carried out. This will enable us to compare theoretical predictions obtained by employing these different approaches and help reveal the role of power corrections at low momentum transfer in the exclusive process under consideration.

In our calculations we use the following values of n_f , Λ and μ_0^2

$$n_f = 3, \Lambda = 0.25 \text{ GeV}, \mu_0^2 = 1 \text{ GeV}^2 \quad (50)$$

and employ both the one angle (11) and the two mixing-angles schemes (13).

In Figs. 1 to 4 the predictions for the FF's $\eta\gamma$ and $\eta'\gamma$ are presented for various values of the input parameters $B_2^g(\eta_1)$, $B_2^g(\eta_8)$ and $B_2^g(\eta_1)$. All of them are found within the one-angle mixing scheme. In Figs. 1 and 2 the (perturbative) HSA predictions are also shown for the sake of comparison. One sees from Fig. 1 that in the framework of the standard mixing scheme, even the asymptotic DA's of the η and η' mesons describe the CLEO data rather well. Though both FF's, especially $Q^2 F_{\eta\gamma}(Q^2)$, are slightly below the data points, their deviations are not so dramatic as to exclude the “pure” asymptotic form of the DA's (i.e.,

³ Notice that in this Section “FF” means the “scaled FF”.

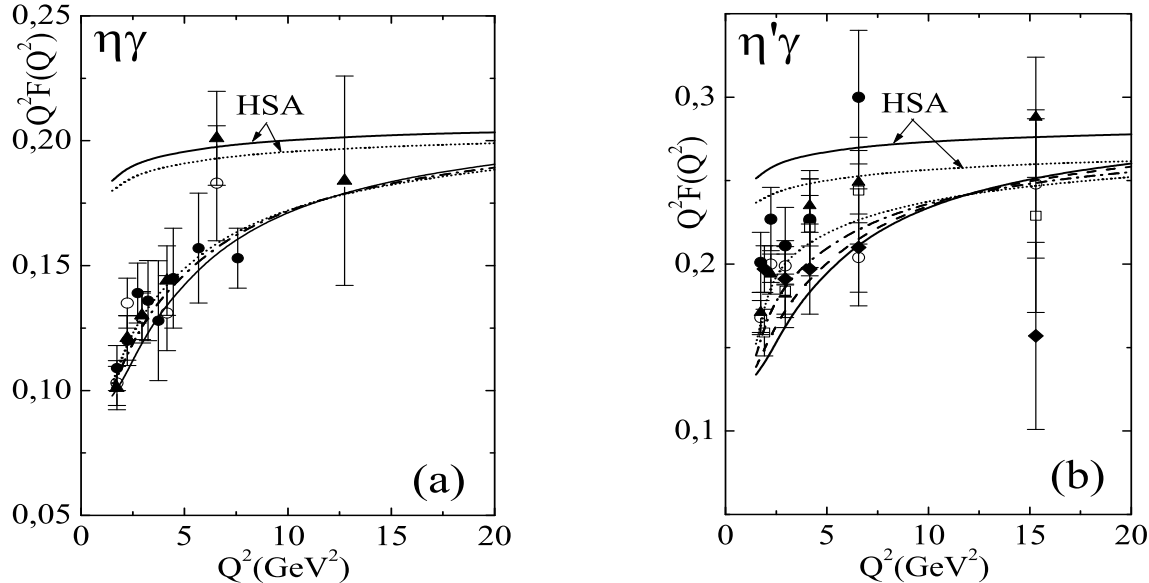


FIG. 2: Scaled transition form factors for $\eta\gamma$ (left) and $\eta'\gamma$ (right) as functions of Q^2 , but using for the calculation of the η_1 and η_8 DA's the parameters $B_2^g(\eta_1) = B_2^g(\eta_8) = 0.05$. The solid curves correspond to $B_2^g(\eta_1) = 0$; the dashed curve in (b) has $B_2^g(\eta_1) = 4$, whereas the dash-dotted curves use $B_2^g(\eta_1) = 10$, and the dotted ones $B_2^g(\eta_1) = 16$.

those with coefficients $B_2^g(\eta_1) = B_2^g(\eta_8) = B_2^g(\eta_1) = 0$. To improve the agreement with the data, some admixture of non-asymptotic terms is required. Indeed, good agreement with the data can be achieved by using DA's with $B_2^g(\eta_1) \neq 0$, $B_2^g(\eta_8) \neq 0$, $B_2^g(\eta_1) = 0$ (see, Figs. 2, 3).

The gluonic contribution to the $\eta\gamma$ and $\eta'\gamma$ transition FF's with $B_2^g(\eta_1) > 0$ further improves this agreement. Numerical calculations demonstrate that this contribution is important at relatively low values of the momentum transfer Q^2 and has the following key features, which we list below:

- The gluonic contribution arising from the η_1 DA with $B_2^g(\eta_1) > 0$ enhances the transition FF's $Q^2 F_{\eta\gamma}(Q^2)$ and $Q^2 F_{\eta'\gamma}(Q^2)$ in the region $1.5 \text{ GeV}^2 \leq Q^2 \leq 12 \text{ GeV}^2$ while reducing them at $Q^2 > 12 \text{ GeV}^2$.
- The gluonic contribution originating from DA's with $B_2^g(\eta_1) < 0$ reduces the form factors in the domain $1.5 \text{ GeV}^2 \leq Q^2 \leq 12 \text{ GeV}^2$ and enhances them beyond $Q^2 > 12 \text{ GeV}^2$.
- The effects described in the previous two items are sizeable for the $\eta'\gamma$ transition FF and for larger values of $B_2^g(\eta_1)$ relative to the $\eta\gamma$ transition FF and using smaller values of $B_2^g(\eta_1)$.

We have also carried out a calculation of the transition FF's using the two-mixing angles parameterization scheme, employing the asymptotic DA's for the η_1 and η_8 states. The FF's found within this scheme lie significantly lower than the data. The deviation is more pronounced for the $\eta\gamma$ transition, originating mainly from a small value of $N_1 f_\eta^1$. Therefore, to correct the picture, relatively large admixtures of the first Gegenbauer polynomial in the

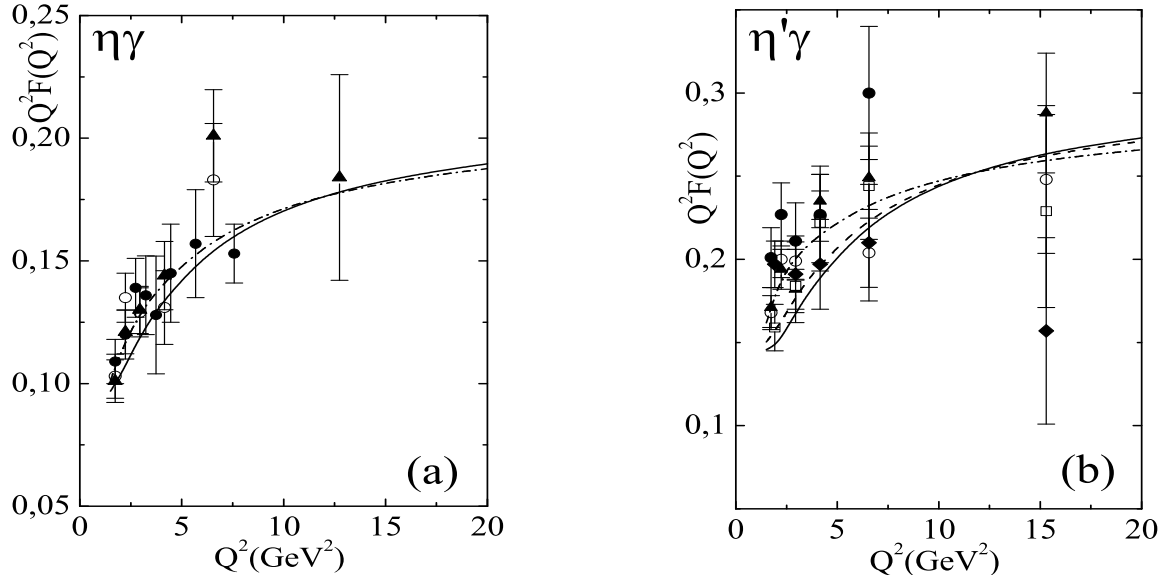


FIG. 3: The $\eta\gamma$ (left) and $\eta'\gamma$ (right) scaled transition form factors as functions of Q^2 , using for all predictions shown the parameters $B_2^q(\eta_1) = 0.1$ and $B_2^q(\eta_8) = 0$. For the solid curves we set $B_2^q(\eta_1) = 0$; the dashed curve in (b) has $B_2^q(\eta_1) = 4$, whereas for the dash-dotted curves we use $B_2^q(\eta_1) = 14$.

DA's of the η_1 and η_8 states are required. In Fig. 5 we depict the FF's obtained using the parameters $B_2^q(\eta_1) = 0.15$, $B_2^q(\eta_8) = 0.15$ and two different values of $B_2^q(\eta_1)$. We consider the values $B_2^q(\eta_1) = B_2^q(\eta_8) = 0.15$ as determining the lower bound for the admissible set of DA's in the context of the two-mixing angles parameterization scheme. In this scheme the negative values of the parameter $B_2^q(\eta_1)$ have to be excluded.

In Sect. III we have emphasized that HT ambiguities produced by the principal value prescription affect the predictions for the transition FF's in accordance with Eq. (42). The HT ambiguity $[Q^2 F_{M\gamma}^{1(8)}(Q^2)]^{HT}$ depends on the η_1 and η_8 DA's and also on the constant $\{N_q\}$. In reality, however, for given DA's of the η_1 and η_8 states, the available experimental information allows one to extract constraints on $\{N_q\}$. To effect the influence of such contributions, we show in Fig. 6, exemplarily also for the others, predictions for the FF's with and without HT ambiguities, using for the expansion coefficients $B_2^q(\eta_1) = B_2^q(\eta_8) = 0.05$, $B_2^q(\eta_1) = 6$. Depending on the values of the constants $\{N_q = \pm 1\}$, the FF's with the HT ambiguities at $Q^2 < 5 \text{ GeV}^2$ are larger (smaller) than the FF's without such corrections and are, in addition, smaller (larger) for $Q^2 > 5 \text{ GeV}^2$. The HT ambiguities do not exceed the level of $\pm 31\%$ of the corresponding FF's in the region $Q^2 \sim 1.2 - 1.5 \text{ GeV}^2$ and reach only $\mp 4\%$ in the region $Q^2 \sim 16 - 20 \text{ GeV}^2$.

Let us pause for a moment to make some important remarks. In accordance with the “ultraviolet dominance hypothesis”, HT corrections to a physical quantity can be estimated using the aforementioned ambiguities. In the present work we take into account only one possible source of power corrections to the $\eta\gamma$, $\eta'\gamma$ transition FF's, namely those arising from the end-point $x \rightarrow 0$; 1 integration. The inclusion of still higher-order HT contributions and higher Fock states to the η and η' meson DA's, may, in principle, further improve the theoretical predictions—as observed, for instance, for the pion electromagnetic form factor

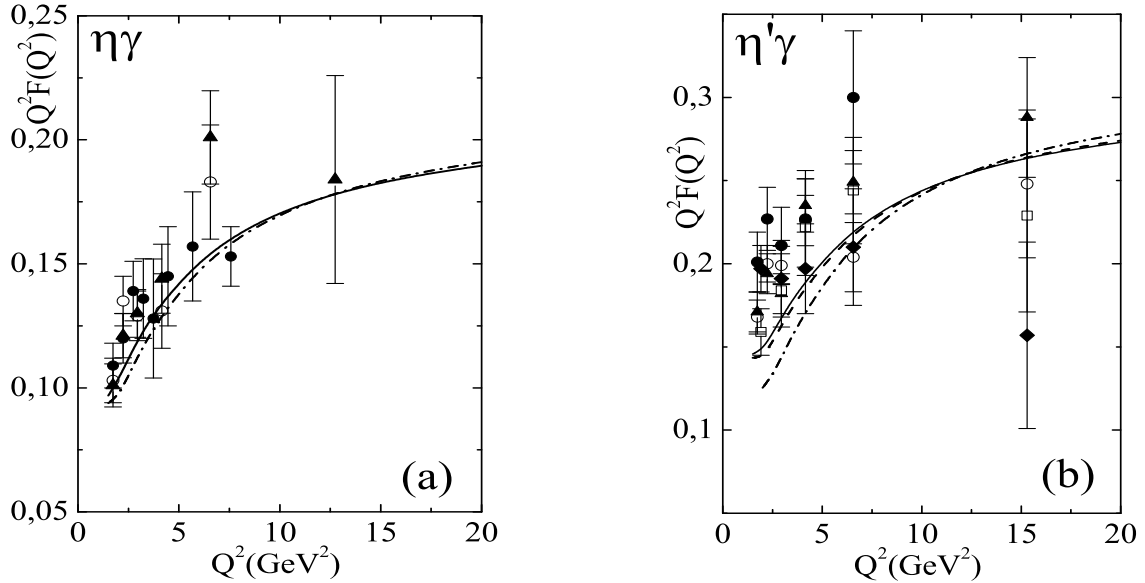


FIG. 4: The $\eta\gamma$ (left) and $\eta'\gamma$ (right) scaled transition form factors as functions of Q^2 , using for all predictions shown the parameters $B_2^q(\eta_1) = 0.1$ and $B_2^q(\eta_8) = 0$. The solid curves correspond to $B_2^g(\eta_1) = 0$; the dashed curve in (b) has $B_2^g(\eta_1) = -2$, whereas for the dash-dotted curves $B_2^g(\eta_1) = -10$ is used.

[33]. Despite the fact that such refinements are beyond the scope of the present investigation, let us estimate the order of magnitude of other HT contributions to the form factors. To this end, we have computed the HT ambiguities associated with the value $\{N_q\} = \pm 0.5$ for $q = 1, 2, 3, 4$, displaying in Fig. 6 the FF's for $\{N_q\} = -0.5$. One observes that these predictions are not in conflict with the data, from which we draw the conclusion that there is still some room for power corrections coming from other sources and that these corrections are not negligible, reaching $\sim \pm(16 - 3)\%$ of the magnitude of the FF's at momentum transfers in the range $Q^2 \sim 1.2 - 2.5$ GeV 2 .

Returning to the results of our analysis, we present the estimates for the eigenfunctions expansion coefficients of the η_1 and η_8 DA's in the context of the ordinary mixing scheme:

$$B_2^q(\eta_1) = 0, B_2^q(\eta_8) = 0, B_2^q(\eta_1) = 4 \div 18, \quad (51)$$

$$B_2^q(\eta_1) = 0.05, B_2^q(\eta_8) = 0.05, B_2^q(\eta_1) = 0 \div 16, \quad (52)$$

and

$$B_2^q(\eta_1) = 0.1, B_2^q(\eta_8) = 0, B_2^q(\eta_1) = -2 \div 14. \quad (53)$$

The constraints (51)–(53) on input parameter $B_2^q(\eta_1)$ are extracted at fixed $B_2^q(\eta_1)$ and $B_2^q(\eta_8)$ and represent the allowed range of values of $B_2^q(\eta_1)$ compatible with the CLEO data. Restrictions on the parameters $B_2^q(\eta_1)$ and $B_2^q(\eta_8)$ at fixed $B_2^q(\eta_1)$ can also be derived. For example, for $B_2^q(\eta_1) = 8$, we get

$$B_2^q(\eta_1) = 8, B_2^q(\eta_1) = 0 \div 0.1, B_2^q(\eta_8) = 0 \div 0.05. \quad (54)$$

On the other hand, in the two-mixing angles scheme, we obtain

$$B_2^q(\eta_1) = 0.15, B_2^q(\eta_8) = 0.15, B_2^q(\eta_1) = 4 \div 20. \quad (55)$$

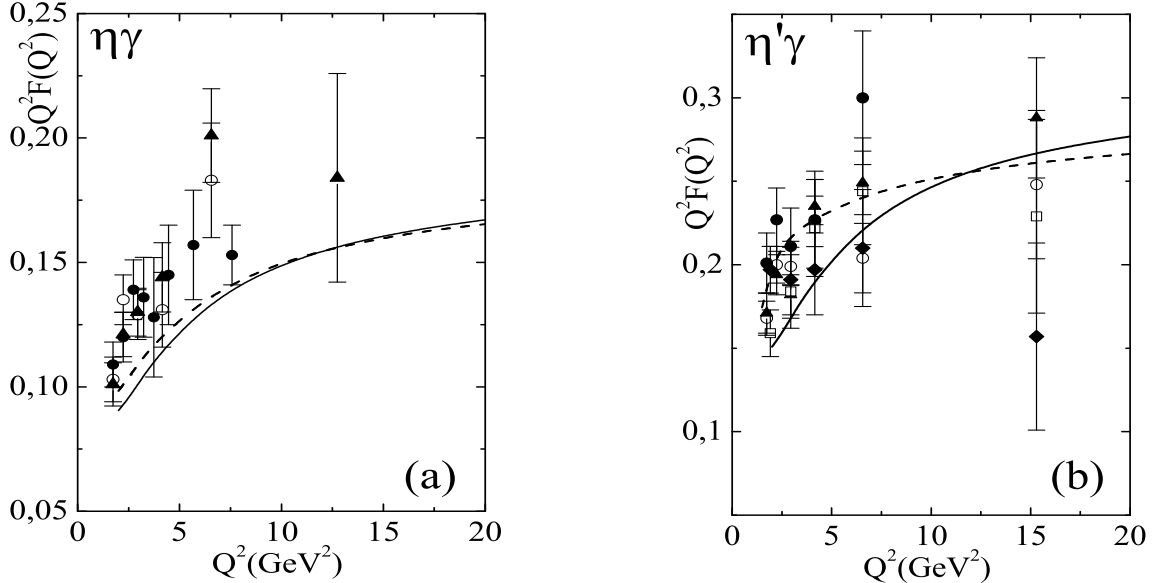


FIG. 5: The $\eta\gamma$ (left) and $\eta'\gamma$ (right) scaled transition form factors vs. Q^2 within the two-mixing angles scheme. All predictions displayed refer to the parameters $B_2^q(\eta_1) = B_2^q(\eta_8) = 0.15$. The solid curves correspond to $B_2^g(\eta_1) = 0$, whereas the dashed curves have $B_2^g(\eta_1) = 20$.

The η and η' DA's were extracted from the CLEO data on the $\eta\gamma$ and $\eta'\gamma$ transition FF's [6] having also recourse to the η' -meson energy spectrum in the decay $\Upsilon(1S) \rightarrow \eta'X$ [34]. In both papers the standard HSA was employed. In Ref. [6], estimates for the parameters $B_2^1(\mu_0^2)$, $B_2^g(\mu_0^2)$ and $B_2^8(\mu_0^2)$ were made within the two-angles mixing scheme (13), reading

$$B_2^1(1 \text{ GeV}^2) = -0.08 \pm 0.04, \quad B_2^g(1 \text{ GeV}^2) = 9 \pm 12, \quad B_2^8(1 \text{ GeV}^2) = -0.04 \pm 0.04. \quad (56)$$

The latter coefficients are related to ours by the expressions

$$B_2^1(\mu_0^2) = \frac{A(\mu_0^2)}{6}, \quad B_2^g(\mu_0^2) = \frac{B(\mu_0^2)}{5}, \quad B_2^8(\mu_0^2) = \frac{C(\mu_0^2)}{6}. \quad (57)$$

Using our approach the values of these parameters are determined to be

$$\begin{aligned} B_2^1(1 \text{ GeV}^2) &= -0.12 \pm 0.08, \quad B_2^g(1 \text{ GeV}^2) = 11 \pm 7, \quad B_2^8(1 \text{ GeV}^2) = 0, \\ B_2^1(1 \text{ GeV}^2) &= -0.039 \pm 0.089, \quad B_2^g(1 \text{ GeV}^2) = 8.16 \pm 8, \quad B_2^8(1 \text{ GeV}^2) = 0.05, \\ B_2^1(1 \text{ GeV}^2) &= 0.033 \pm 0.087, \quad B_2^g(1 \text{ GeV}^2) = 6.32 \pm 8, \quad B_2^8(1 \text{ GeV}^2) = 0, \end{aligned} \quad (58)$$

and

$$B_2^1(1 \text{ GeV}^2) = -0.04 \pm 0.05, \quad B_2^g(1 \text{ GeV}^2) = 8 \pm 0.16, \quad B_2^8(1 \text{ GeV}^2) = 0.025 \pm 0.025. \quad (59)$$

One appreciates that within the ordinary mixing scheme, $B_2^8(1 \text{ GeV}^2) \geq 0$ while $B_2^1(1 \text{ GeV}^2)$ can have either a positive or also a negative sign.

In the case of the two-mixing angles scheme, we find

$$B_2^1(1 \text{ GeV}^2) = 0.017 \pm 0.088, \quad B_2^g(1 \text{ GeV}^2) = 12.48 \pm 8, \quad B_2^8(1 \text{ GeV}^2) = 0.15. \quad (60)$$

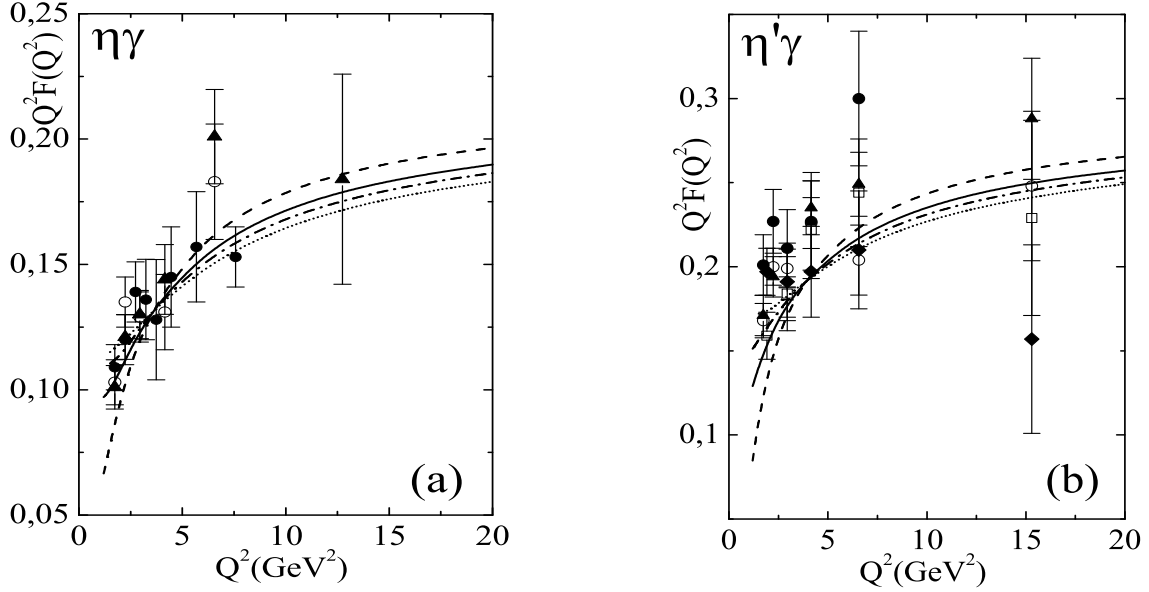


FIG. 6: The $\eta\gamma$ (left) and $\eta'\gamma$ (right) scaled transition form factors as functions of Q^2 . All predictions have been obtained within the ordinary mixing scheme. The DA's of η and η' refer to the parameters $B_2^g(\eta_1) = B_2^g(\eta_8) = 0.05$ and $B_2^g(\eta_1) = 6$. The broken lines denote the FF's with the HT uncertainties included via Eq. 42 employing the following values of $\{N_q\}$, $q = 1, 2, 3, 4 : 1$ (dashed lines); -1 (dotted lines); -0.5 (dash-dotted lines).

Now $B_2^8(1 \text{ GeV}^2) > 0$ and the coefficient $B_2^1(1 \text{ GeV}^2)$ is preferably positive (cf. Eq. (56)).

On the other hand, the constraints for the parameters $B_2^g(\mu_0^2)$ and $B_2^g(\mu_0^2)$ extracted in Ref. [34] at the normalization point $\mu_0^2 = 2 \text{ GeV}^2$ read

$$B_2^g(2 \text{ GeV}^2) = 0.010 \pm 0.068, \quad B_2^g(2 \text{ GeV}^2) = 5.6 \pm 3.4. \quad (61)$$

Comparing now Eq. (61) with the values given in Eqs. (55), and taking into account that in Ref. [34] different values for the scheme parameters defined by Eq. (50) were used, we come to the conclusion that in the context of the RC method the region $B_2^g(2 \text{ GeV}^2) < 0$ should be excluded as contradicting to the CLEO data.

The apparent discrepancy between the results of the present work and those of Ref. [6] concerning the extracted values of the coefficients $B_2^1(1 \text{ GeV}^2)$ and $B_2^8(1 \text{ GeV}^2)$ is connected to the fact that the employed theoretical schemes are intrinsically different. Indeed, the transition FF's found in the standard HSA tend to overestimate the CLEO data (see Figs. 1 and 2). The DA's with parameters $B_2^g(\eta_1), B_2^g(\eta_8) > 0$ even increase this disagreement, whereas by adding the gluon component with $B_2^g(\eta_1) > 0$ one can reduce it. Therefore, to decrease the magnitude of the FF's and achieve this way a better agreement with the data, one has to allow for DA's with $B_2^g(\eta_1), B_2^g(\eta_8) < 0$. The power corrections change this situation radically. In fact, at low-momentum transfer they enhance the absolute value of the NLO correction to the FF's more than by a factor of 2 – 2.5 and because the contribution of the NLO term to the FF's is negative, power corrections reduce the leading-order prediction for the FF's considerably, while at the highest Q^2 values measured by the CLEO collaboration this influence becomes more moderate. As a result, the input parameters, extracted from the CLEO data using the RC method obey the restrictions $B_2^g(\eta_1), B_2^g(\eta_8), B_2^g(\eta_1) > 0$. In

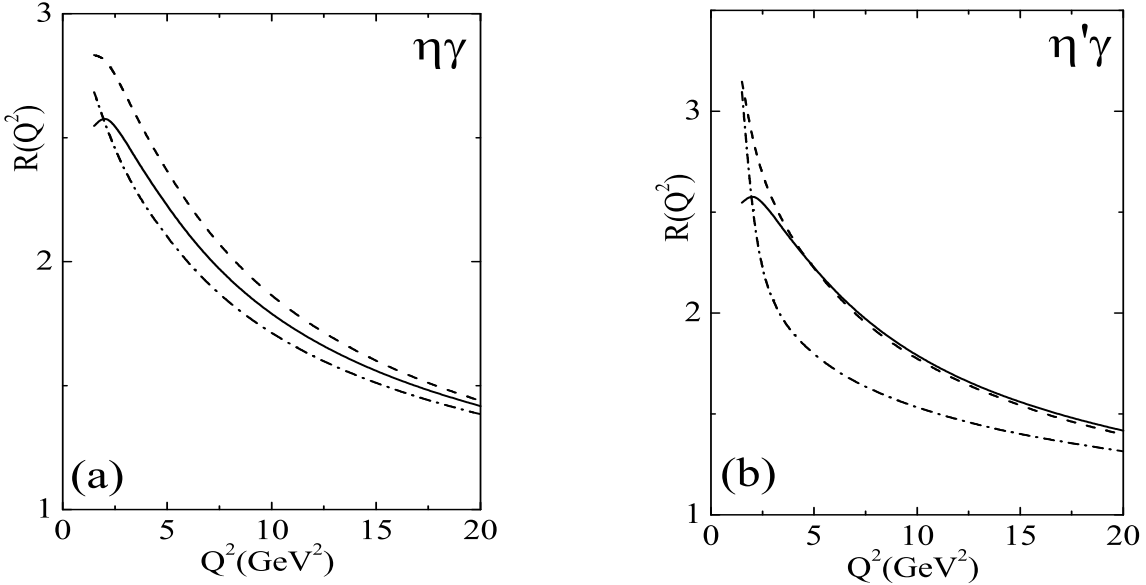


FIG. 7: The form-factor ratio $R(Q^2)$, given by Eq. (62), for the $\eta\gamma$ (a) and $\eta'\gamma$ (b) electromagnetic transition. The solid lines correspond to the input parameters $B_2^q(\eta_1) = B_2^q(\eta_8) = B_2^g(\eta_1) = 0$. The dash-dotted lines describe the same ratio for $B_2^q(\eta_1) = B_2^q(\eta_8) = 0$, $B_2^g(\eta_1) = 14$ and the dashed ones for $B_2^q(\eta_1) = B_2^q(\eta_8) = 0.05$, $B_2^g(\eta_1) = 10$.

order to quantify these statements, we show in Fig. 7 the numerical results for the ratio

$$R_{M\gamma}(Q^2) = \frac{[Q^2 F_{M\gamma}(Q^2)]_{NLO}^{res}}{[Q^2 F_{M\gamma}(Q^2)]_{NLO}^{HSA}} \quad (62)$$

for some values of the expansion coefficients.

V. CONCLUDING REMARKS

In this work we have performed a computation of the $\eta\gamma$ and $\eta'\gamma$ transition FF's within the RC method. The latter has enabled us to estimate a class of power corrections to the FF's, namely precisely those owing to the end-point $x \rightarrow 0$, 1 integrations in the corresponding pQCD factorization formulas. Contributions to the FF's from the quark as well as the gluon components of the η and η' mesons have been taken into account. We have obtained the Borel resummed expressions $[Q^2 F_{M\gamma}(Q^2)]^{res}$ for the FF's and proved that in the asymptotic limit $Q^2 \rightarrow \infty$ they lead to the standard HSA predictions.

We have demonstrated that the effect of these power corrections on the $\eta\gamma$ and $\eta'\gamma$ transition FF's is considerable. Indeed, at moderate values of the momentum transfer $Q^2 \leq 5$ GeV 2 they turn out to enhance the absolute value of the $O(\alpha_s)$ correction to the FF's more than $R_{M\gamma}(Q^2) = 2\text{-}2.5$ times. The factor $R_{M\gamma}(Q^2)$ depends on the specific $M\gamma$ transition under consideration and on the input parameters (expansion coefficients in the eigenfunction basis) of the η and η' meson DA's. Thus, at different values of $B_2^q(\eta_1)$, $B_2^q(\eta_8)$ and $B_2^g(\eta_1)$ the ratio $R_{M\gamma}$ is rather stable for the $\eta\gamma$ transition, whereas it is rather sensitive in the case of the $\eta'\gamma$ one. These features of the power corrections have important consequences: the enhanced NLO correction significantly reduces the leading-order contribution to the FF's so

that the input parameters of the η and η' meson DA's, which correctly describe the CLEO data within the RC method, must obey the constraints (51)–(53) and (55). It is worth emphasizing that our predictions for the η and η' meson DA's disagree with those extracted from the CLEO data in the context of the standard HSA.

Moreover, the performed analysis has also provided us the means to estimate the magnitude of HT corrections to the FF's, originating from sources other than the end-point integrations. To achieve that goal, we have used the “ultraviolet dominance hypothesis” and estimated the HT corrections employing uncertainties generated by the principal value prescription. It turns out that such corrections may be sizeable at low Q^2 and should be therefore taken into account.

The DA's of the η and η' mesons obtained in this work can be useful in the investigation of other exclusive processes that involve η and η' mesons, especially at lower momentum-transfer values.

[1] S. S. Agaev, Phys. Rev. D **64**, 014007 (2001).

[2] S. S. Agaev and A. I. Mukhtarov, Int. J. Mod. Phys. A **16**, 3179 (2001).

[3] J. Cao, F.-G. Cao, T. Huang, and B.-Q. Ma, Phys. Rev. D **58**, 113006 (1998) [hep-ph/9807508].

[4] R. Jakob, P. Kroll, and M. Raulfs, J. Phys. G **22**, 45 (1996) [hep-ph/9410304]; P. Kroll and M. Raulfs, Phys. Lett. B **387**, 848 (1996); Th. Feldmann and P. Kroll, Eur. Phys. J. C **5**, 327 (1998) [hep-ph/9711231]; M. Diehl, P. Kroll, and C. Vogt, Eur. Phys. J. C **22**, 439 (2001) [hep-ph/0108220].

[5] N. G. Stefanis, W. Schroers, and H. C. Kim, Phys. Lett. B **449**, 299 (1999) [hep-ph/9807298]; Eur. Phys. J. C **18**, 137 (2000) [hep-ph/0005218].

[6] P. Kroll and K. Passek-Kumerički, Phys. Rev. D **67**, 054017 (2003) [hep-ph/0210045].

[7] A. Khodjamirian, Eur. Phys. J. C **6**, 477 (1999) [hep-ph/9712451].

[8] A. Schmedding and O. Yakovlev, Phys. Rev. D **62**, 116002 (2000) [hep-ph/9905392].

[9] A. P. Bakulev, S. V. Mikhailov, and N. G. Stefanis, Phys. Rev. D **67**, 074012 (2003) [hep-ph/0212250]; hep-ph/0303039.

[10] Y. V. Mamedova, Int. J. Mod. Phys. A **18**, 1023 (2003).

[11] CLEO Collaboration, J. Gronberg et al., Phys. Rev. D **57**, 33 (1998) [hep-ex/9707031].

[12] M. K. Chase, Nucl. Phys. **B174**, 109 (1980); V. N. Baier and G. Grozin, Nucl. Phys. **B192**, 476 (1981); M. V. Terentyev, Sov. J. Nucl. Phys. **33**, 911 (1981) [Yad. Fiz. **33**, 1692 (1981)].

[13] S. S. Agaev and N. G. Stefanis, hep-ph/0212318.

[14] G. P. Lepage and S. J. Brodsky, Phys. Rev. D **22**, 2157 (1980); A. V. Efremov and A. V. Radyushkin, Phys. Lett. B **94**, 245 (1980); Theor. Math. Phys. **42**, 97 (1980) [Teor. Mat. Fiz. **42**, 147 (1980)]; A. Duncan and A. H. Mueller, Phys. Rev. D **21**, 1636 (1980).

[15] S. S. Agaev, Phys. Lett. B **360**, 117 (1995) [Erratum-ibid, B **369**, 379 (1996)]; [hep-ph/9611215].

[16] S. S. Agaev, Mod. Phys. Lett. A **10**, 2009 (1995); ibid. A **11**, 957 (1996); ibid. A **13**, 2637 (1998) [hep-ph/9805278].

[17] D. V. Shirkov and I. L. Solovtsov, Phys. Rev. Lett. **79**, 1209 (1997) [hep-ph/9704333].

[18] A. I. Karanikas and N. G. Stefanis, Phys. Lett. B **504**, 225 (2001) [hep-ph/0101031].

[19] N. G. Stefanis, in 8th Adriatic Meeting and Central European Symposia on Particle Physics in the New Millennium, Dubrovnik, Croatia, 4-14 Sep. 2001, to appear in Lect. Notes Phys. by Springer Verlag [hep-ph/0203103].

[20] F. del Aguila and M. K. Chase, Nucl. Phys. **B193**, 517 (1981); E. Braaten, Phys. Rev. D **28**, 524 (1983); E. P. Kadantseva, S. V. Mikhailov, and A. V. Radyushkin, Sov. J. Nucl. Phys. **44**, 326 (1986) [Yad. Fiz. **44**, 507 (1986)].

[21] B. Melić, B. Nižić, and K. Passek, Phys. Rev. D **65**, 053020 (2002) [hep-ph/0107295].

[22] Th. Feldmann, P. Kroll, and B. Stech, Phys. Rev. D **58**, 114006 (1998) [hep-ph/9802409].

[23] A. P. Bakulev, S. V. Mikhailov and N. G. Stefanis, Phys. Lett. B **508**, 279 (2001) [hep-ph/0103119]; in *Proceedings of the 36th Rencontres de Moriond on QCD and Hadronic Interactions, 17-24 Mar 2001, Les Arcs, France*, 133-136 [hep-ph/0104290].

[24] A. P. Bakulev and S. V. Mikhailov Phys. Rev. D **65**, 114511 (2002) [hep-ph/0203046].

[25] V. Y. Petrov et al., Phys. Rev. D **59**, 114018 (1999) [hep-ph/9807229] M. Praszalowicz and A. Rostworowski, Phys. Rev. D **64**, 074003 (2001) [hep-ph/0105188].

[26] S. J. Brodsky, G. P. Lepage, and P. B. Mackenzie, Phys. Rev. D **25**, 228 (1983).

- [27] M. Beneke, Phys. Rep. **317**, 1 (1999) [hep-ph/9807443].
- [28] P. Gosdzinsky and N. Kivel, Nucl. Phys. **B521**, 274 (1998) [hep-ph/9707367].
- [29] S. V. Mikhailov, Phys. Lett. B **431**, 387 (1998) [hep-ph/9804263].
- [30] E. Braaten and Y.-Q. Chen, Phys. Rev. D **57**, 4236 (1998), [Erratum-ibid. D **59**, 079901 (1999)] [hep-ph/9710357].
- [31] R. Akhoury, A. Sinkovics, and M. G. Sotiropoulos, Phys. Rev. D **58**, 013011 (1998) [hep-ph/9709497].
- [32] A. P. Prudnikov, Yu. A. Brychkov, and O. I. Marichev, Integrals and Series, Vol. 3; More Special Functions (Gordon and Breach, New York, 1990).
- [33] V. M. Braun, A. Khodjamirian, and M. Maul, Phys. Rev. D **61**, 073004 (2000) [hep-ph/9907495].
- [34] A. Ali and A. Ya. Parkhomenko, hep-ph/0304278.